

# Complexation in Asymmetric Solutions of Oppositely Charged Polyelectrolytes: Phase Diagram

Nikolay N. Oskolkov and Igor I. Potemkin\*

Physics Department, Moscow State University, Moscow 119992, Russian Federation; Department of Polymer Science, University of Ulm, Ulm 89069, Germany

Received April 20, 2007; Revised Manuscript Received August 7, 2007

**ABSTRACT:** We propose a combination of the mean-field theory and the random phase approximation to describe complexation in solutions of oppositely charged polyelectrolytes with the asymmetric content of positively and negatively charged chains. The phase diagram of the system is calculated. We show that “excess” polyions coexisting with small neutral complexes (each complex consists of one polycation and one polyanion) at very small polymer concentrations can first aggregate into big spherical clusters with the following formation of cylindrical and lamellar structures at the increase of polymer concentration. All clusters formed have nonzero net charge due to the charge asymmetry of the solution. The physical reason for the stability of the clusters (complexes) is discussed.

## 1. Introduction

Water-soluble complexes are known to be formed by a number of synthetic and natural oppositely charged polyelectrolytes.<sup>1–8</sup> An unique peculiarity of such systems is that the opposite tendencies, such as intermolecular aggregation and solubility of the complexes, have a common electrostatic origin. It is believed that the short-range attraction of charged units is mediated by thermodynamic fluctuations of the charges (relatively weak electrostatic interactions similarly with those of the Debye–Hückel plasma) or by strong multipole (dipole, quadrupole, etc.) interactions of associated charged groups. On the other hand, solubility of the complexes can be attributed to the existence of the long-range electrostatic forces due to the local violation of electric neutrality of the system. That is why such systems are very sensitive to variation of pH and salt concentration. For example, the screening of the electrostatic forces via adding of the low-molecular-weight salt induces destruction of the complexes.<sup>2</sup>

Up to now theoretical studies of oppositely charged linear polyelectrolytes were mainly focused on the effect of precipitation, i.e., macroscopic phase separation induced by the electrostatic attraction.<sup>9–13</sup> Stability of finite-size complexes was predicted for the case of macromolecules that form a micellar (core–shell) structure.<sup>14–19</sup> Here solubility of the micelles is provided by hydrophilic blocks forming corona of the micelle. For example, in dilute solution of polyelectrolyte/neutral diblock copolymers and oppositely charged linear chains the core of the micelles is formed by polyelectrolyte complexes between the oppositely charged polyions while the hydrophilic uncharged blocks of the block copolymers comprise the micellar corona.<sup>15,16</sup> Also, micelle formation is predicted for solutions of asymmetric diblock polyampholytes (copolymers having oppositely charged blocks) where complexed segments of the diblocks form the core of the micelle and noncomplexed tails of the longer blocks form the corona.<sup>17,18</sup> A theory of complexation of oppositely charged homopolymers differing in the length predicts stability of the so-called tadpole complexes consisting of a neutral part (head) and of a charged tail.<sup>20</sup> Recent computer simulations showed that in asymmetric solution of

oppositely charged homopolymers (all molecules have the same length and absolute value of the charge density, while the numbers of positively and negatively charged chains are different), nearly homogeneous spherical complexes can be formed.<sup>21–23</sup> It was shown that the lower is the asymmetry, the higher is the size of the complexes.

In the present paper we propose a theory that predicts thermodynamic stability of spatially *homogeneous* spherical, cylindrical, and lamellar complexes in asymmetric solution of oppositely charged homopolymers. A phase diagram including coexistence regions is presented. The physical reason for stability of the complexes is discussed.

## 2. Model

Let us consider a solution of  $N$  linear flexible macromolecules consisting of  $N_+$  polycations (PCs) and  $N_-$  polyanions (PAs),  $N_+ + N_- = N$ . We will examine a weakly asymmetric solution,  $N_+ > N_-$ , when an asymmetry parameter  $A$  is small enough,  $A = (N_+ - N_-)/N \ll 1$ . For the sake of simplicity we assume that each macromolecule comprises  $m$  segments, each of the size  $a$ , and has a small fraction of charged groups  $f = 1/\sigma \ll 1$ . Each charged group carries an elementary charge  $e$ . Also we assume that only  $N_+ - N_-$  “excess” PCs have counterions to provide a macroscopic electric neutrality of the system while counterions coming from  $N_-$  PAs and  $N_-$  PCs are “washed away”. The solvent is considered to be a  $\Theta$ -solvent for neutral segments of both kinds of macromolecules.

In very dilute solution (but above the complexation concentration threshold), one can imagine stability of two states of the solution: (i) all “neutralizing” PCs aggregate with PAs and form neutral PC–PA globules (each globule consists of one PC and one PA) that freely float in the solution together with the excess PCs, and (ii) all neutral globules precipitate forming a macrophase. Keeping in mind that attraction between the globules is induced by the short-range electrostatic interactions, we can expect that stability of the single globules is possible if the fraction of charged groups is not so high.

The total free energy (per unit volume) of the mixture of the globules and excess PCs has a form

$$\mathcal{F}_{\text{PCs+glob}} = \frac{\phi A}{m} F_{\text{PC}} + \frac{\phi(1-A)}{2m} F_{\text{glob}} \quad (1)$$

\* To whom correspondence should be addressed. E-mail: igor@polly.phys.msu.ru.

where  $F_{PC}$  and  $F_{glob}$  are the free energies of the polycation and the globule, respectively;  $\phi \ll 1$  is the average polymer volume fraction in the solution. For derivation of  $F_{PC}$ , we use the so-called two zone Oosawa model:<sup>24–26</sup>

$$\begin{aligned} \frac{F_{PC}}{k_B T} = & \frac{3}{10} \frac{l_B t(\theta)}{r} \left( \frac{m}{\sigma} (1 - \beta) \right)^2 + \frac{m\beta}{\sigma} \ln \left( \frac{\psi\beta}{\sigma} \right) + \\ & \frac{m(1 - \beta)}{\sigma} \ln \left( \frac{\psi}{\sigma} \frac{\phi A (1 - \beta)}{\psi - \phi A} \right) + \frac{3}{2} \frac{r^2}{ma^2} + mC\psi^2 + \ln \left( \frac{\phi A}{m} \right) \\ t(\theta) = & \frac{2 - 3\theta^{1/3} + \theta}{(1 - \theta)^2}, \theta = \left( \frac{r}{r_0} \right)^3 = \frac{\phi A}{\psi} \end{aligned} \quad (2)$$

In this model, the total volume of the system  $V$  is imagined as a set of  $N_+ - N_-$  densely packed, neutral spheres (cells) of the radius  $r_0$ ,  $V \approx (N_+ - N_-)4\pi r_0^3/3$ . Each cell is divided into two zones. The first zone that is approximated by a sphere of the radius,  $r$ , is occupied by the PC. The second zone of the volume  $4\pi(r_0^3 - r^3)/3$  is free of the PC. Counterions are distributed inhomogeneously between the zones because of inhomogeneous distribution of the charge of the PC within the cell. This distribution is approximated by a steplike function: the fraction  $\beta$  of the counterions occupies the first zone so that the number of the counterions within the PC is equal to  $\beta m/\sigma$ . The resultant volume charge density of the PC is assumed to be constant and equal to  $\rho_{in} = em(1 - \beta)/(\sigma 4\pi r^3/3)$ . The second zone is charged with the density  $\rho_{out} = -em(1 - \beta)/(\sigma 4\pi(r_0^3 - r^3)/3)$  due to electric neutrality of the cell. Calculation of the Coulomb energy of the concentric spheres with constant charge densities can be done in a standard way<sup>26</sup> resulted in the first term of eq 2. Here  $l_B$  is the Bjerrum length,  $l_B = e^2/\epsilon k_B T$ , and  $\epsilon$  is the dielectric constant of the solvent. The next two terms of eq 2 are the contributions of the translational motion of counterions;  $\psi = mv/(4\pi r^3/3)$  is the polymer volume fraction inside the PC, and  $v \approx a^3$  is the excluded volume of the counterion that coincides with the excluded volume of the monomer unit. The fourth term of eq 2 is the elastic free energy of the chain taken in the Flory form, and the next term takes into account triple interactions of monomer units in the  $\Theta$ -solvent,  $C \sim 1$  is the dimensionless third virial coefficient. Finally, the last term of eq 2 corresponds to the translational entropy of the PCs. The equilibrium value of  $F_{PC}$  is found by minimization with respect to the parameters  $\beta$  and  $r$  (or  $\psi$ ).

It has to be noted that the spherical approximation for the first zone (for the conformation of the PC) is reasonable for relatively wide range of values of  $f = 1/\sigma$ . Indeed, if the fraction of the charged groups is very small, the electrostatic repulsion between the charges (or the osmotic pressure of counterions inside the chain) weakly disturb the isotropic Gaussian conformation of the chain, i.e., the volume of the chain can be approximated by a sphere. If  $f$  is relatively high, the chain attains an elongated conformation that can be viewed as sequence of the electrostatic blobs<sup>27</sup> (counterions-free regime). Then the free energy of the chain is proportional to the number of blobs and scales as  $F_{PC}/k_B T \approx m(l_B/a)^{2/3}/\sigma^{4/3}$ . The same value of the free energy of the PC,  $F_{PC}/k_B T \approx 0.9 \cdot 5^{1/3} m(l_B/a)^{2/3}/\sigma^{4/3}$ , can be found from eq 2 by minimization with respect to  $r$ , if we neglect localization of the counterions inside the PC ( $\beta = 0$ ) and the energy of the excluded volume interactions, and if we set  $\theta = 0$  ( $\phi A \ll \psi$ ). Thus, relying on the correct result in counterions-free approximation, we believe that the spherical approximation is the more accurate under inclusion of counterion localization ( $\beta \neq 0$ ).

The total free energy of the neutral globule formed by one PC and one PA takes the following form:

$$\begin{aligned} \frac{F_{glob}}{k_B T} = & \frac{2m}{\psi} \left[ C\psi^3 + \frac{\sqrt{2}}{12\pi} \left( \frac{48\psi\pi l_B}{\sigma^2 a} \right)^{3/4} \right] + \gamma 4\pi R^2 + \\ & \ln \frac{\phi(1 - A)}{2m} + 2 \ln \frac{\psi}{m} - \ln 2, \quad \psi = \frac{2mv}{4\pi R^3/3} \end{aligned} \quad (3)$$

The first two terms  $\sim m$  are the volume contributions to the free energy of the globule. Notice that formation of the globule cannot be described within the mean-field approximation: the Coulomb term is equal to zero at this level. One has to include at least fluctuations around the electroneutral state to describe the complexation. The simplest way to do it is the RPA formalism.<sup>17,28–30</sup> The RPA free energy is given in the square brackets of eq 3. The first term describes hard core repulsive interactions of monomer units in the  $\Theta$ -solvent. The second term is the RPA correction to the mean-field free energy. It is responsible for the fluctuation-induced attraction of charged units. Calculation of this term is done in Appendix A.

The third term  $\sim m^{2/3}$  is the surface energy of the globule,  $\gamma$  is the surface tension coefficient (divided by  $k_B T$ ). Finally, the first and the next two logarithmic terms are the entropic contributions of translational motion of the globules and chains within the globule, respectively. An equilibrium value of  $F_{glob}$  is derived by minimization of eq 3 with respect to  $\psi$ . In the case of high enough fraction of the charged groups,  $f \gg (a/l_B)^{1/2} m^{-3/4}$ , the volume free energy is dominant, and  $F_{glob}$  can be calculated using a perturbation theory.

Calculation of the surface tension coefficient  $\gamma$  is done in the Appendix B:

$$\gamma \approx 0.11 \frac{u^{2/3}}{\sigma^{4/3} a^2}, \quad u = \frac{l_B}{a} \quad (4)$$

Notice that this result coincides with the result of the scaling theory.<sup>18</sup> Thus, eqs 1–4 completely describe the free energy of the mixture of the excess PCs and the globules.

The free energy of the excess PCs coexisting with precipitated globules (a dense macrophase),  $\mathcal{F}_{PCs+prec}$ , is also done by eq 1 where  $F_{glob}$  does not comprise the surface tension energy and the entropic terms are reduced to the single one, equal to  $2 \ln(\psi/m)$ .

There is a question as to whether the excess polycations can form a complex with the neutral globules. It turns out that weakly charged finite-size globules can be stable. This, at first sight the unusual phenomenon, can be explained on a following example. Let us assume that we have two spherical droplets differing in the size: the smaller one of the radius  $r$  carries a charge  $q$ , and the bigger one of the radius  $R$ ,  $R \gg r$ , is neutral. The electrostatic energy of the droplets is  $\approx q^2/r$ . Let us also assume that the droplets can merge with each other forming a single droplet whose charge is distributed over the whole volume. Then the electrostatic energy of this droplet is  $\approx q^2/R < q^2/r$ ; i.e., the merging is energetically favorable. Therefore, if we deal with one excess PC and many neutral globules, their complexation to a charged globule can also energetically be favorable.<sup>30,32</sup> Furthermore, the stretching of the excess PC decreases after complexation due to the screening of the electrostatic interactions;<sup>30</sup> i.e., the elasticity of the PC also stabilizes the charged globule. Therefore, we can expect that homogeneous solution of charged, optimum-size globules can be stable. By analogy with the microdomains known for associating polyelectrolytes,<sup>26</sup> we consider the formation of

spherical, cylindrical and lamellar complexes. The derivation of the free energy of weakly charged complexes can also be done within the two-zone Oosawa model:

$$\begin{aligned} \mathcal{F}_d = & \frac{\phi}{\psi} \left[ d \frac{\gamma' a^3}{R} + \frac{2\pi u}{5} \left( \frac{\psi A (1-\beta)}{\sigma} \right)^2 \frac{R^2}{a^2} t_d(\theta) + \right. \\ & \frac{\psi A}{\sigma} \beta \ln \left( \frac{\psi A}{\sigma} \beta \right) + \frac{\psi A}{\sigma} (1-\beta) \ln \left( \frac{\psi A}{\sigma} \frac{\phi(1-\beta)}{\psi - \phi} \right) + \frac{3}{2} \frac{\psi^{1/3}}{m^{4/3}} + \\ & \left. C\psi^3 + \frac{\sqrt{2}}{12\pi} \left( \frac{48\psi\pi l_B}{\sigma^2 a} \right)^{3/4} + \frac{\psi}{m} \ln \left( \frac{\psi}{m} \right) + \frac{1}{V_d} \ln \left( \frac{\phi}{\psi V_d} \right) \right] \\ d = & 1 \text{ (lamellae), } 2 \text{ (cylinders), } 3 \text{ (spheres)} \quad (5) \end{aligned}$$

where

$$\begin{aligned} t_1(\theta) = \frac{5}{3\theta}, \quad t_2(\theta) = \frac{5}{4} \frac{\theta - 1 - \ln \theta}{(1-\theta)^2}, \\ t_3(\theta) = \frac{2 - 3\theta^{1/3} + \theta}{(1-\theta)^2}, \quad \theta = \frac{\phi}{\psi} < 1 \end{aligned}$$

$$V_1 = 2RS/a^3, \quad V_2 = \pi R^2 L/a^3, \quad V_3 = \frac{4\pi}{3} R^3/a^3, \quad S, L \rightarrow \infty$$

The first term in square brackets of eq 5 is the surface energy of the complex. The second term is the mean-field electrostatic energy calculated under assumption that all excess charge is homogeneously “smeared” throughout the volume of the complex;  $\beta$  is the fraction of counterions inside the complex. Taking into account that the fraction of the excess PCs is small,  $A \ll 1$ , and that all neutralizing PCs are mobile, such an assumption is quite reasonable. The next two terms are the entropic contributions of translational motion of counterions. The fifth and the sixth terms correspond to the elastic free energy of the chains and to the excluded volume energy in  $\Theta$ -solvent, respectively. The seventh term of eq 5 is the RPA correction to the Coulomb free energy responsible for the short-range attraction of charged units (derivation of this term for the case of charged complex is done in ref<sup>30</sup>). The last two terms of eq 5 correspond to the translational entropy of the chains within the clusters and of the clusters as whole objects, respectively. The last contribution is nonzero only for the case of spherical clusters. An equilibrium value of the free energy  $\mathcal{F}_d$  is derived by minimization with respect to the polymer volume fraction of the cluster,  $\psi$ , fraction of the counterions within the cluster,  $\beta$ , and the radius (hemithickness) of the cluster,  $R$ .

Finally, if the polymer concentration is high enough, coalescence of the charged globules into macroscopic complex has to occur. The free energy of this state is derived from eq 5 by setting  $\beta = 1$ :

$$\begin{aligned} \mathcal{F}_{\text{macro}} = & \frac{\phi A}{\sigma} \ln \left( \frac{\phi A}{\sigma} \right) + \frac{3}{2} \frac{\phi^{1/3}}{m^{4/3}} + C\phi^3 + \frac{\sqrt{2}}{12\pi} \left( \frac{48\phi\pi l_B}{\sigma^2 a} \right)^{3/4} + \\ & \frac{\phi}{m} \ln \left( \frac{\phi}{m} \right) \quad (6) \end{aligned}$$

### 3. Results and Discussion

A simplified  $\sigma$ - $\phi$  phase diagram of the solution that does not take into account coexistence of different phases, can be constructed by comparison of the free energies,  $\mathcal{F}_{\text{PCs+glob}}$ ,  $\mathcal{F}_{\text{PCs+prec}}$ ,  $\mathcal{F}_{\text{macro}}$ , and  $\mathcal{F}_d$ ,  $d = 1, 2, 3$ , Figure 1.

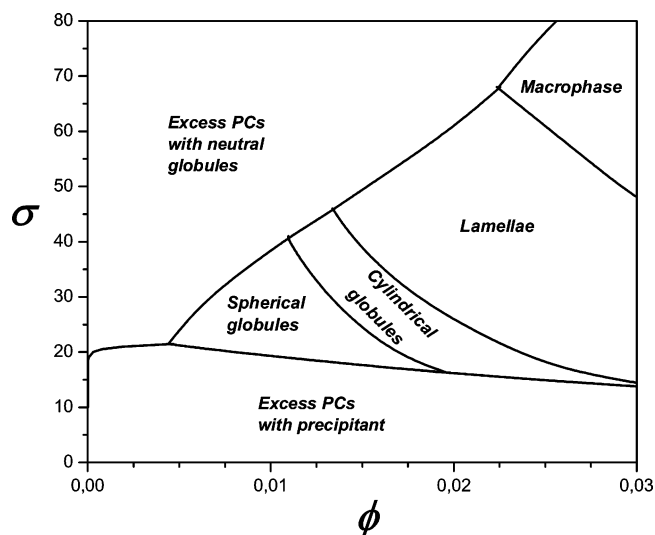


**Figure 1.** Simplified  $\sigma$  -  $\phi$  phase diagram obtained by equating of the free energies at fixed values of the parameters  $m = 10^4$ ,  $A = 0.01$ , and  $u = 1$ .

As we expected, the excess PCs do not aggregate with the neutral globules at low values of polymer volume fraction: they are mixed with the globules (small values of the fraction of the charged groups  $f = 1/\sigma$ ) or coexist with the precipitant (high values of  $f$ ). However, charged spherical, cylindrical and lamellar complexes (globules) are stable at intermediate values of  $\phi$  and  $\sigma$ . The predicted sequence of the transitions—spheres, cylinders, and lamellae—with the increase of  $\phi$  is mainly determined by the dependence of the Coulomb energy on  $\phi$  (on the distance between the clusters). We can see in eq 5 that the Coulomb energy of the spheres has the lowest value at small values of  $\theta = \phi/\psi$  ( $t_3 \rightarrow \text{const}$ ),  $t_2$  has a weak logarithmic dependence,  $t_2 \sim -\ln \theta$ , and  $t_1$  has a strong dependence on  $\theta$ ,  $t_1 \sim 1/\theta$ . In other words,  $t_3 \ll t_2 \ll t_1$  at  $\theta \ll 1$ , i.e. the spherical globules have the lowest Coulomb energy. On the other hand, the opposite inequalities are held for the surface tension energy (first term of eq 5): this energy is lowest for the lamellar complexes. Therefore, at small values of  $\phi$  only spherical globules can be stable because of the lower Coulomb energy. The increase of  $\phi$  decreases Coulomb energy of the cylindrical and lamellar structures and due to the surface energy, these structures are stabilized.

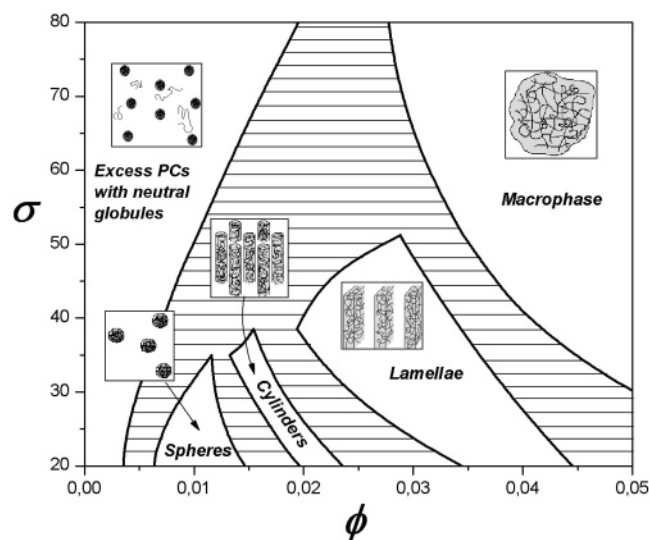
A real phase diagram is obtained by equating the chemical potentials and the osmotic pressures of various phases  $i$  and  $j$ ;  $i, j = \text{PCs} + \text{glob}, 1, 2, 3, \text{macro}$ :

$$\begin{aligned} \mu_i(\phi_1) &= \mu_j(\phi_2) \\ \pi_i(\phi_1) &= \pi_j(\phi_2) \quad (7) \end{aligned}$$

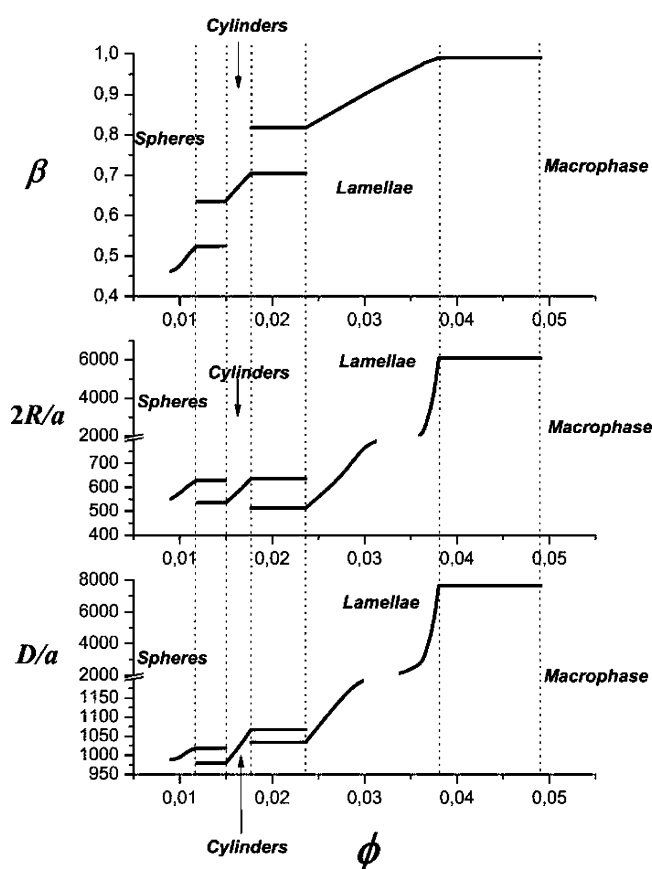
The chemical potential and the osmotic pressure of a phase are calculated in a standard way:

$$\mu_i(\phi) = \frac{\partial \mathcal{F}_i}{\partial \phi}, \quad \pi_i(\phi) = \phi \mu_i(\phi) - \mathcal{F}_i \quad (8)$$

Here  $\mathcal{F}_i$  are obtained by the use of eqs 1, 5, and 6. In eq 7,  $\phi_1$  and  $\phi_2$  are the average polymer volume fractions of coexisting phases. The numerical solution of eq 7 is plotted in Figure 2. The shaded area corresponds to the coexistence of various phases. We can see that location of the stability regions of the charged globules (spheres, cylinders, and lamellae) correspond to the simplified diagram, Figure 1. In addition, coexistence of

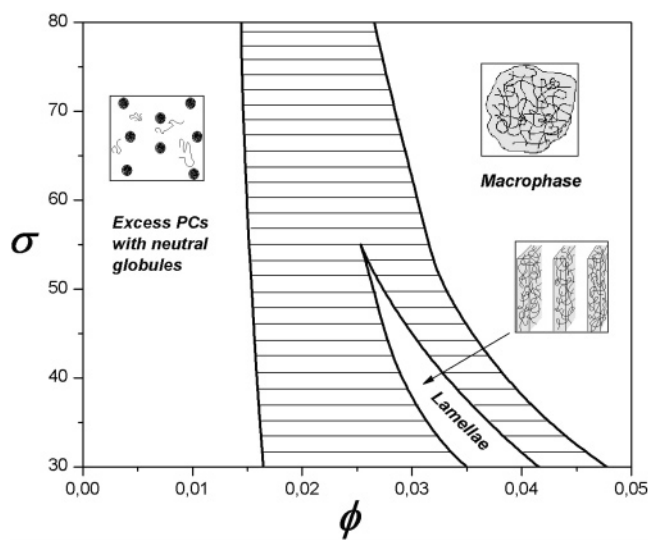


**Figure 2.**  $\sigma$ - $\phi$  phase diagram of the solution of oppositely charged polyelectrolytes.  $A = 0.01$ ,  $m = 10^4$ , and  $u = 1$ .



**Figure 3.** Fraction of counterions within the charged complexes,  $\beta$ , the diameter (thickness) of the charged complexes,  $2R$ , and the distance between the complexes,  $D = 2R(\psi/\phi)^{1/d}$ ,  $d = 1$  (lamellae),  $2$  (cylinders),  $3$  (spheres) vs  $\phi$ .  $A = 0.01$ ,  $m = 10^4$ ,  $u = 1$ , and  $\sigma = 30$ .

the spheres with the cylinders, the cylinders with the lamellae, and the lamellae with the macrophase is possible. The phase of the neutral globules with excess PCs can coexist with all other phases. The width of the coexistence region of the homogeneous mixture of PCs with the neutral globules and of the macrophase narrows with the increase of  $\sigma$ , Figure 2. This effect is related to the weakening of the electrostatic attraction between the chains.



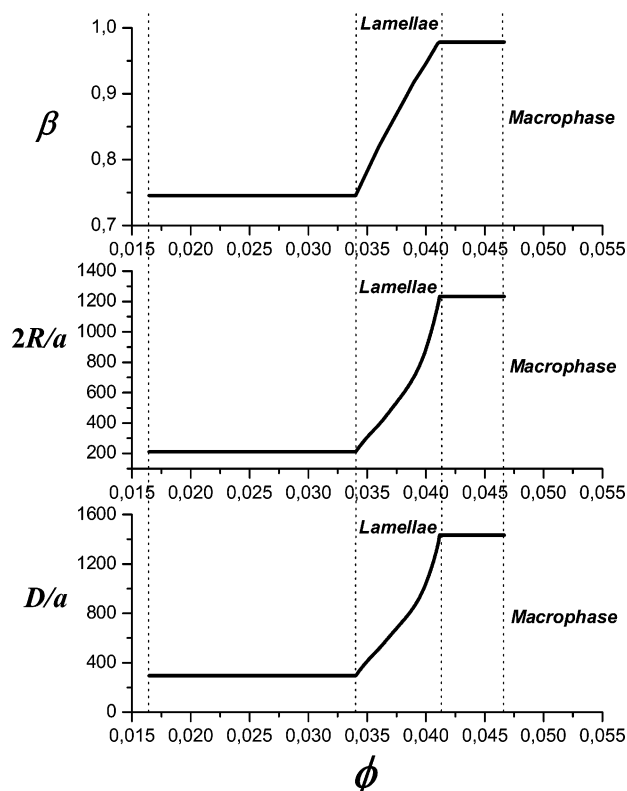
**Figure 4.**  $\sigma$ - $\phi$  phase diagram of the solution of oppositely charged polyelectrolytes.  $A = 0.03$ ,  $m = 10^4$ , and  $u = 1$ .

Figure 3 represents dependencies of the fraction of counterions within the charged complexes,  $\beta$ , the diameter (thickness) of the complexes,  $2R$ , and the characteristic distance between them,  $D = 2R(\psi/\phi)^{1/d}$ ,  $d = 1$  (lamellae),  $2$  (cylinders),  $3$  (spheres) on the average polymer volume fraction. In the single-phase regions, all these parameters are the increasing functions of  $\phi$ . The increase of  $\beta$  with  $\phi$  is related to the growth of the size of the complex which is accompanied by the growth of its bare charge. The counterions condensation prohibits enhancement of the electrostatic energy of the complex. The  $\beta$ - $\phi$  plot depicts also that maximum, medium and minimum values of  $\beta$  correspond to the lamellar, cylindrical and spherical complexes, respectively. Such relation is explained by a value of the electrostatic energy of bare (counterions-free) complexes which is maximum for the lamellae. The horizontal lines in Figure 3 correspond to the coexistence regions. Independence of  $\beta$ ,  $R$ , and  $D$  on  $\phi$  in the coexistence region is due to the constant densities of the coexisting phases: in accordance with the Maxwell's rule, the increase of the average polymer volume fraction  $\phi$  results in variation of the volumes of the phases whereas the densities of them remain constant. A peculiarity of the phase transitions induced by the increase of  $\phi$  is that each "new" phase has thinner complexes coexisting with the thicker ones of the "old" phase, Figure 3.

Phase behavior of the solution is very sensitive to variation of the asymmetry parameter  $A$ . For example, a triple increase of the parameter suppresses stability of the spherical and cylindrical complexes and narrows the stability region of the lamellar structure, Figure 4. Disappearance of the charged globules at small values of polymer concentration is related to the release of counterions which are localized within the globule. Such release is favorable entropically. That is why coexistence of the excess PCs with the neutral complexes is more favorable in this regime. Notice that we confine ourselves by the analysis of weakly asymmetric solutions,  $A \ll 1$ , and examination of coexistence of the excess PCs with charged globules at  $A \leq 1$  is outside the scope of the model.

The increase of  $A$  makes the lamellae thinner and decreases the distance between them. For example,  $2R/a \approx 1680$  and  $D/a \approx 2350$  at  $A = 0.01$ ,  $\phi = 0.035$  while  $2R/a \approx 315$  and  $D/a \approx 420$  at  $A = 0.03$ ,  $\phi = 0.035$ , Figure 5.

Our calculations are consistent with recent computer simulations<sup>21-23</sup> where stability of charged spherical complexes



**Figure 5.** Fraction of counterions within the lamellar complexes,  $\beta$ , the thickness of the lamellae,  $2R$ , and the distance between the lamellae,  $D = 2R(\psi/\phi)$ , vs  $\phi$ .  $A = 0.03$ ,  $m = 10^4$ ,  $u = 1$ , and  $\sigma = 30$ .

was shown. It has been demonstrated that large complexes are formed when excess of one kind of polyion decreases.

Our predictions of the stability of the spherical complexes are also in qualitative agreement with experimental results.<sup>3,4,7</sup> The structure of polyelectrolyte complexes between poly(sodium styrenesulfonate) and copolymers of diallyldimethylammonium chloride and acrylamide was studied by viscometry, static and dynamic light scattering, and electron microscopy.<sup>3</sup> In diluted, nonstoichiometric solutions, polyelectrolyte complex formation leads to polydisperse systems of highly aggregated, nearly spherical particles of  $R_h \approx 140 \div 460$  nm (depending on the fraction of charged groups of the copolymer). At a 1:1 molar mixing ratio, flocculation occurs.

The complex formation in the oppositely charged linear and flexible polyelectrolytes: quaternized poly(vinylpyridinium) (QPVP) and poly(sodium styrenesulfonate) was investigated by static and dynamic light scattering, flow birefringence, and viscometry over a wide range of mixing ratios  $0.003 \leq m \leq 0.9$  (the ratio of the number of charges on PAs to the total number of charges on PAs and PCs).<sup>4</sup> The observed clusters were stable and had average dimensions  $R_g \approx R_h \approx 100$  nm at low and high mixing ratios. As the mixing ratio approached  $m \approx 0.4$ , which corresponds to the gel point, the number and the dimensions of clusters grew to  $R \approx 150\text{--}300$  nm. According to the flow birefringence data, the axial ratio of the clusters at the gel point  $m \approx 0.4$  was 1.07, which corresponds to the spherical shape.

Kinetics of complex formation of nonviral DNA with poly-L-lysine was studied in ref 7 by time-resolved multiangle laser light scattering, which yields the time evolution of the supramolecular complex mass and geometric size. Primary complexes whose geometric size is smaller than individual DNA molecules in solution were formed very rapidly upon mixing DNA and

poly-L-lysine. Over time, these primary complexes aggregated into larger structures whose ultimate size was determined primarily by the relative concentrations of DNA and poly-L-lysine. The maximum complex size occurred at a DNA/poly-L-lysine charge ratio near unity.

#### 4. Conclusion

In conclusion, we proposed a theory of complexation in asymmetric solution of oppositely charged linear polyelectrolytes. Flexible polycations and polyanions of equal length and fraction of charged groups were examined. We predicted stability of spatially homogeneous (over)charged complexes (globules) that are spherical, cylindrical, or lamellar. A phase diagram of the solution is constructed.

**Acknowledgment.** Financial support of the Deutsche Forschungsgemeinschaft within the SFB 569, the Russian Foundation for Basic Research, and the Russian Agency for Science and Innovations is gratefully acknowledged.

#### Appendix A

Let us consider a neutral PA–PC complex which is free of counterions. The physical reason for attraction in the complex is that the thermodynamic fluctuations of polymer density provide local violation of the electric neutrality of the complex, and emerging positively and negatively charged regions (virtual “dipoles”) attract each other. That is why the free energy density functional has to comprise the electrostatic term. Assuming weakness of the density fluctuations, the free energy functional of the complex can be written in Gaussian approximation as  $F_{\text{vol}} = F_0 + \delta F$ , where  $F_0/k_B T = 2mC\psi^2$  and

$$\frac{\delta F(\xi_+, \xi_-)}{k_B T} = \frac{1}{2} \int \frac{d\mathbf{q}}{(2\pi)^3} \left[ \frac{4\pi l_B}{q^2} \left| \frac{\xi_+(\mathbf{q})}{\sigma} - \frac{\xi_-(\mathbf{q})}{\sigma} \right|^2 + v \frac{a^2 q^2}{6\psi} (|\xi_+(\mathbf{q})|^2 + |\xi_-(\mathbf{q})|^2) + 6vC\psi \left| \xi_+(\mathbf{q}) + \xi_-(\mathbf{q}) \right|^2 \right] \quad (9)$$

In this expression  $\xi_{\pm}(\mathbf{q})$  are Fourier transformed small density fluctuations of monomer units of the PC and PA;  $\mathbf{q}$  is the wave vector, and  $|\xi_{\pm}(\mathbf{q})|^2 \equiv \xi_{\pm}(\mathbf{q})\xi_{\pm}(-\mathbf{q})$ .

The first term of eq 9 corresponds to the electrostatic interactions. It vanishes in the limit  $q \rightarrow 0$  because of the electric neutrality of the complex. The second term is the conventional structural (entropic) contribution<sup>31</sup> (translational motion of PC and PA is neglected). Finally, the third term comes from the energy of the volume interactions.

The contribution of the fluctuating charges to the free energy of the complex can be found following a standard procedure:

$$\frac{F_{\text{RPA}}}{k_B T} = - \ln \int \mathcal{D}\xi_+ \mathcal{D}\xi_- \exp \left\{ - \frac{\delta F(\xi_+, \xi_-)}{k_B T} \right\} + \ln \int \mathcal{D}\xi_+ \mathcal{D}\xi_- \exp \left\{ - \frac{\delta F(\xi_+, \xi_-)}{k_B T} \right\}_{l_B=0} \quad (10)$$

Here  $\mathcal{D}\xi_+ \mathcal{D}\xi_- \equiv \prod_{\mathbf{q}} d\xi_+(\mathbf{q}) d\xi_-(\mathbf{q})$  is a product of differentials.

One of the possible ways to calculate the Gaussian integrals in eq 10 is the substitution of the continuous integration over the wave vector  $\mathbf{q}$ , eq 9, by a discrete summation over the wave numbers  $\mathbf{k}$ ,  $\mathbf{q} = 2\pi\{k_x/L_x, k_y/L_y, k_z/L_z\}$ ,  $k_x, k_y, k_z = 0, \pm 1, \pm 2,$

..., where  $\mathcal{L}_{x,y,z}$  are the linear dimensions of the system,  $\mathcal{L}_x \mathcal{L}_y \mathcal{L}_z = V_c$

$$\frac{\delta F(\xi_+, \xi_-)}{k_B T} = \frac{1}{2V_c} \sum_{\mathbf{k}} \left[ \frac{4\pi l_B}{q_k^2} \left| \frac{\xi_+(\mathbf{k})}{\sigma} - \frac{\xi_-(\mathbf{k})}{\sigma} \right|^2 + \frac{a^2 q_k^2}{6\psi} (|\xi_+(\mathbf{k})|^2 + |\xi_-(\mathbf{k})|^2) + 6vC\psi \left| \xi_+(\mathbf{k}) + \xi_-(\mathbf{k}) \right|^2 \right] \quad (11)$$

$$q_k^2 \equiv (2\pi)^2 \left( \frac{k_x^2}{\mathcal{L}_x^2} + \frac{k_y^2}{\mathcal{L}_y^2} + \frac{k_z^2}{\mathcal{L}_z^2} \right)$$

Then the expressions in the logarithms of eq 10 are infinite products of integrals over variables  $\xi_{\pm}(\mathbf{k})$ . Diagonalization of the square form, eq 11, can be done via the following variable substitution

$$\xi_+(\mathbf{k}) = \eta_+(\mathbf{k}) + \xi_-(\mathbf{k}) \frac{\frac{4\pi l_B}{q_k^2 \sigma^2} - 6vC\psi}{\frac{4\pi l_B}{q_k^2 \sigma^2} + v \frac{a^2 q_k^2}{6\psi} + 6vC\psi} \quad (12)$$

$$\frac{\delta F(\eta_+, \xi_-)}{k_B T} = \frac{1}{2V_c} \sum_{\mathbf{k}} \left[ \left| \eta_+(\mathbf{k}) \right|^2 \left( \frac{4\pi l_B}{q_k^2 \sigma^2} + v \frac{a^2 q_k^2}{6\psi} + 6vC\psi \right) + \left| \xi_-(\mathbf{k}) \right|^2 \frac{\left( v \frac{a^2 q_k^2}{6\psi} + 12vC\psi \right) \left( v \frac{a^2 q_k^2}{6\psi} + \frac{8\pi l_B}{q_k^2 \sigma^2} \right)}{\frac{4\pi l_B}{q_k^2 \sigma^2} + v \frac{a^2 q_k^2}{6\psi} + 6vC\psi} \right] \quad (13)$$

Using the well-known result for the Gaussian integral

$$\int_{-\infty}^{\infty} dx \exp(-\beta x^2) = \sqrt{\frac{\pi}{\beta}} \quad (14)$$

and integrating the exponents over  $\eta_+(\mathbf{k})$  and  $\xi_-(\mathbf{k})$ , we obtain

$$\begin{aligned} \frac{F_{\text{RPA}}}{k_B T} &= -\ln \prod_{\mathbf{k}} \sqrt{\frac{\frac{a^2 q_k^2}{v} + \frac{8\pi l_B}{q_k^2 \sigma^2}}{\frac{a^2 q_k^2}{6\psi} + \frac{8\pi l_B}{q_k^2 \sigma^2}}} \\ &= \frac{1}{2} \sum_{\mathbf{k}} \ln \left( 1 + \frac{48\pi l_B \psi}{v a^2 q_k^4 \sigma^2} \right) \\ &= \frac{V_c}{2} \frac{\int d\mathbf{q}}{(2\pi)^3} \ln \left( 1 + \frac{48\pi l_B \psi}{v a^2 q^4 \sigma^2} \right) \end{aligned} \quad (15)$$

where we have returned from summation to integration. Equation 15 comprises both the energy of fluctuation-induced interactions between the charges and the electrostatic self-energy of the chains. In contrast to the systems with low-molecular-weight ions,<sup>33,34</sup> the integral in eq 15 is convergent at  $q \rightarrow \infty$ :

$$\frac{F_{\text{RPA}}}{k_B T V_c} = \frac{\sqrt{2}}{12\pi} \left( \frac{48\pi \psi l_B}{v \sigma^2 a^2} \right)^{3/4} \quad (16)$$

Despite a positive value,  $F_{\text{RPA}}$  is responsible for the electrostatic attraction, because  $F_{\text{RPA}} = \text{const}/\psi^{1/4}$  ( $V_c = 2mv/\psi$ ); i.e.,  $F_{\text{RPA}}$  decreases with the increase of  $\psi$ .

## Appendix B

Calculation of the surface tension coefficient of the complex can be done via minimization of the one-dimensional functional:

$$\gamma = \int_{-\infty}^{+\infty} dx \left[ \frac{a^2}{v} \frac{(\psi'(x))^2}{24 \psi(x)} + C\psi(x)^3 + \frac{\sqrt{2}}{12\pi} \left( \frac{48\pi \psi(x) l_B}{\sigma^2 a} \right)^{3/4} + \mu \psi(x) \right] \quad (17)$$

over the polymer volume fraction,  $\psi(x)$ , that depends on the normal coordinate  $x$  in vicinity of the surface. It is assumed that  $\psi(x)$  monotonously changes from 0 in pure solvent (at  $x = -\infty$ ) to some constant value  $\psi_0$  inside the complex far from the surface (at  $x = +\infty$ ). Therefore, obvious boundary conditions imposed on  $\psi(x)$  are  $\psi(-\infty) = 0$ ,  $\psi(+\infty) = \psi_0$ , and all derivatives (first, second, etc.) of  $\psi(x)$  over  $x$  at  $x = \pm\infty$  are equal to zero,  $\psi'(\pm\infty) = \psi''(\pm\infty) = \dots = 0$ . The first term of eq 17 is the conventional gradient term<sup>31</sup> that describes entropic losses of the chains because of inhomogeneous density near the surface. The next two terms are the coordinate-dependent contributions to the volume free energy of the globule, and the last term is introduced to take into account normalization of  $\psi(x)$ ;  $\mu$  is the Lagrange multiplier.

Minimization of the functional (17) can be done in a standard way using substitution  $\psi(x) = y(x)^2$ :

$$-\frac{a^2}{3} y''^2 + 6C y^5 + \frac{\sqrt{2}}{12\pi} \left( \frac{48\pi l_B}{\sigma^2 a} \right)^{3/4} \frac{3}{2} y^{1/2} + 2\mu y = 0 \quad (18)$$

The boundary conditions are

$$\begin{aligned} y(-\infty) &= 0, y(+\infty) = y_0 = \sqrt{\psi_0} \\ y'(\pm\infty) &= y''(\pm\infty) = \dots = 0 \end{aligned} \quad (19)$$

Equation 18 can be integrated after multiplying by  $y'$ :

$$-\frac{a^2}{6} (y')^2 + C y^6 + \frac{\sqrt{2}}{12\pi} \left( \frac{48\pi l_B}{\sigma^2 a} \right)^{3/4} y^{3/2} + \mu y^2 = 0 \quad (20)$$

where the constant of integration is set equal to zero due to the boundary conditions at  $x = -\infty$ . Applying the boundary conditions at  $x = +\infty$  to eqs 18 and 20, we get

$$y_0 = \left( \frac{\sqrt{2}}{96\pi C} \left( \frac{48\pi l_B}{\sigma^2 a} \right)^{3/4} \right)^{2/9}, \mu = -9C y_0^4 \quad (21)$$

Using eq 20, one can present the surface tension coefficient as follows:

$$\begin{aligned}\gamma &= \int_{-\infty}^{+\infty} \frac{dx}{v} \cdot \frac{a^2(y')^2}{3} = \frac{a^2 y_0}{3v_0} \int_0^{y_0} dy y' = \\ &= \frac{a\sqrt{6}}{3v_0} \int_0^{y_0} dy \sqrt{C y^6 + \frac{\sqrt{2}}{12\pi} \left( \frac{48\pi l_B}{\sigma^2 a} \right)^{3/4} y^{3/2} + \mu y^2} \\ &= \frac{a\sqrt{6} C y_0^4}{3v_0} \int_0^1 dt \sqrt{t^6 + 8t^{3/2} - 9t^2} \approx 0.11 \frac{u^{2/3}}{\sigma^{4/3} a^2} \quad (22)\end{aligned}$$

where  $u = l_B/a$  and  $C = 1$ .

## References and Notes

- (1) Bakeev, K. N.; Izumrudov, V. A.; Kuchanov, S. I.; Zezin, A. B.; Kabanov, V. A. *Macromolecules* **1992**, *25*, 4249.
- (2) Kabanov, A. V.; Bronich, T. K.; Kabanov, V. A.; Yu, K.; Eisenberg, A. *Macromolecules* **1996**, *29*, 6797.
- (3) Dautzenberg, H.; Hartmann, J.; Grunewald, S.; Brand, F. *Ber. Bunsen-Ges. Phys. Chem.* **1996**, *100*, 1024.
- (4) Pogodina, N. V.; Tsvetkov, N. V. *Macromolecules* **1997**, *30*, 4897.
- (5) Dautzenberg, H. *Macromolecules* **1997**, *30*, 7810.
- (6) Gohy, J.-F.; Varshney, S. K.; Jerome, R. *Macromolecules* **2001**, *34*, 3361.
- (7) Lai, E.; van Zanten, J. H. *Biophys. J.* **2001**, *80*, 864.
- (8) Etrych, T.; Leclercq, L.; Boustta, M.; Vert, M. *Eur. J. Pharmacol. Sci.* **2005**, *25*, 281.
- (9) Overbeek, J. T. G.; Voorn, M. J. *J. Cell Comp. Physiol.* **1957**, *49*, 7.
- (10) Castelnovo, M.; Joanny, J.-F. *Eur. Phys. J. E* **2001**, *6*, 377.
- (11) Kudlay, A.; de la Cruz, M. O. *J. Chem. Phys.* **2004**, *120*, 404.
- (12) Biesheuvel, P. M.; Cohen Stuart, M. A. *Langmuir* **2004**, *20*, 2785.
- (13) Allen, R. J.; Warren, P. B. *Langmuir* **2004**, *20*, 1997.
- (14) Castelnovo, M. *Europhys. Lett.* **2003**, *62*, 841.
- (15) Kramarenko, E. Yu.; Khokhlov, A. R.; Reineker, P. *J. Chem. Phys.* **2003**, *119*, 4945.
- (16) Kramarenko, E. Yu.; Khokhlov, A. R.; Reineker, P. *J. Chem. Phys.* **2006**, *125*, 194902.
- (17) Castelnovo, M.; Joanny, J.-F. *Macromolecules* **2002**, *35*, 4531.
- (18) Shusharina, N. P.; Zhulina, E. B.; Dobrynin, A. V.; Rubinstein, M. *Macromolecules* **2005**, *38*, 8870.
- (19) Wang, Z.; Rubinstein, M. *Macromolecules* **2006**, *39*, 5897.
- (20) Zhang, R.; Shklovskii, B. I. *Physica A* **2005**, *352*, 216.
- (21) Hayashi, Y.; Ullner, M.; Linse, P. *J. Chem. Phys.* **2002**, *116*, 6836.
- (22) Hayashi, Y.; Ullner, M.; Linse, P. *J. Phys. Chem. B* **2003**, *107*, 8198.
- (23) Hayashi, Y.; Ullner, M.; Linse, P. *J. Phys. Chem. B* **2004**, *108*, 15266.
- (24) Oosawa, F. *Polyelectrolytes*; Marcel Dekker: New York, 1971.
- (25) Dobrynin, A. V.; Rubinstein, M. *Macromolecules* **2001**, *34*, 1964.
- (26) Limberger, R. E.; Potemkin, I. I.; Khokhlov, A. R. *J. Chem. Phys.* **2003**, *119*, 12023.
- (27) de Gennes, P. G.; Pincus, P.; Velasco, R. M.; Brochard, F. *J. Phys. (Paris)* **1976**, *37*, 1461.
- (28) Borue, V. Yu.; Erukhimovich, I. Ya. *Macromolecules* **1988**, *21*, 3240.
- (29) Borue, V. Yu.; Erukhimovich, I. Ya. *Macromolecules* **1990**, *23*, 3625.
- (30) Oskolkov, N. N.; Potemkin, I. I. *Macromolecules* **2006**, *39*, 3648.
- (31) Lifshitz, I. M. *Sov. Phys. JETP* **1968**, *55*, 2408.
- (32) Potemkin, I. *Europhys. Lett.* **2004**, *68*, 487.
- (33) Potemkin, I. I.; Khokhlov, A. R. *J. Chem. Phys.* **2004**, *120*, 10848.
- (34) Potemkin, I. I.; Oskolkov, N. N.; Khokhlov, A. R.; Reineker, P. *Phys. Rev. E* **2005**, *72*, 021804.

MA0709304